Open Research Online

The Open University's repository of research publications
and other research outputs

Diffusion bonding of copper alloy to nickel-based superalloy: effect of heat treatment on the microstructure and mechanical properties of the joints

Journal Item

How to cite:

Zhang, Chengcong and Shirzadi, Amir A. (2021). Diffusion bonding of copper alloy to nickel-based superalloy: effect of heat treatment on the microstructure and mechanical properties of the joints. Science and Technology of Welding and Joining (Early Access).

For guidance on citations see FAQs.

© 2021 Institute of Materials, Minerals and Mining

https://creativecommons.org/licenses/by-nc-nd/4.0/

Version: Accepted Manuscript

Link(s) to article on publisher's website:
http://dx.doi.org/doi:10.1080/13621718.2021.1882653

Copyright and Moral Rights for the articles on this site are retained by the individual authors and/or other copyright owners. For more information on Open Research Online's data policy on reuse of materials please consult the policies page.

oro.open.ac.uk

Diffusion bonding of copper alloy to nickel-based superalloy: effect of heat treatment on the microstructure and mechanical properties of the joints

Chengcong Zhang [a*], Amir A. Shirzadi [b,c]

a. Technical Centre, Shanghai Aerospace Equipment Manufacturer, Shanghai 200245, China;

b. School of Engineering & Innovation, The Open University, Milton Keynes, MK7 6AA, UK;

c. School for Materials and Metallurgy, Wuhan University of Science and Technology, Wuhan 430081, China

*Email:： zhangcc0202@163.com

Diffusion bonding of copper alloy to nickel-based superalloy: effect of heat treatment on the microstructure and mechanical properties of the joints

Successful joining of heat conducting materials, such as copper, to high-temperature components is of significant importance for heat management in nuclear power plants and liquid propellant launch vehicles. However, it is impossible to fusion weld copper alloys to stainless steels or nickel superalloys (GH4169) using conventional welding processes. Therefore, solid-state processes, such as friction welding or diffusion bonding, are considered for joining such un-weldable dissimilar materials. Diffusion bonding of a copper alloy (C18150) to a Ni-based superalloy (GH4169) was investigated in this work. The bonding trials at 900°C for 60 minutes under a constant 10 MPa pressure led to formation of sound joints free from intermetallic, pores, voids and discontinuities. Conventional tensile testing led to the failure within the copper alloy and away from the joint (i.e. fully cohesive failure) in all samples. Due to the softening of the copper alloy during the bonding process, the maximum tensile strength of the as-bonded copper alloy was only 48 % of its as-received strength. Post-bonding solution treatment at 960°C for 60min followed by ageing at 450 °C for 3.5 h, restored the tensile strength of the copper alloy up to 77%. The microstructures of the diffusion bonded samples in the as-bonded and after the hardening heat treatment were also investigated.

Key words
Diffusion bonding, Joining, Copper alloy, Nickel-based superalloy, Heat treatment

1. Introduction

Copper alloys are vastly used in heat management systems due to their high thermal conductivities [1]. Joining of copper alloy to structural materials (i.e. stainless steel or Ni-based superalloy) is of significant interest in nuclear power plants [2] and liquid propellant launch vehicles [3]. The combustion chamber of liquid propellant launch vehicles consists of an inner wall made of copper alloys containing cooling channels and an outer wall made of high-strength stainless steels or superalloys. The entire assembly is effectively a pressure vessel which should withstand very high combustion pressures during the lift-off stage of

propellant launch spacecrafts [4].

Many researchers have attempted joining of copper alloy to stainless steel. Previous work shows CuCrZr alloy and 316L stainless steel were successfully joined using hot isostatic pressing (HIP) and explosive welding [2]. Nevertheless, the high temperature of HIP processing (~ 1000℃) resulted in the diffusion-driven changes in the compositions of both alloys and even grain coarsening in the copper alloy. The explosive welding is complex and not readily available process which has its own drawbacks.

Prior work was focused mostly on diffusion bonding of copper alloys to stainless steels [2,4–7]. Diffusion bonding is a solid-state process, which is performed at an elevated temperature but below the melting point of the materials and under a compressive load. This leads to inter diffusion of atoms across the faying interface and consequent bond formation. Temperature, pressure and holding time are the three key factors which must be determined and optimised based on the materials being joined [8]. The temperature is normally between 0.7 to 0.9 of the melting points (in Kelvin) of the base material with the lower melting temperature. In the previous studies, 800℃ to 950℃ was proved to be the optimum temperature when diffusion bonding copper alloys to stainless steels [4,7,9,10].

Generally, direct diffusion bonding of dissimilar materials is a challenging task due to the following reasons [11–13]:

1) Mismatch in the coefficient of thermal expansions (CTE) of dissimilar materials might result in the development of high residual stresses and poor mechanical properties of the joints;

2) Difference in intrinsic diffusion coefficients of alloying elements might lead to formation of micro-voids and micro-cracks at the bonding interface, *i.e.* known as Kirkendall effect;

3) Formation of hard and brittle intermetallic compounds at the joint interface is a common problem when diffusion bonding dissimilar materials.

Although diffusion bonding of copper to stainless steels has been well researched, a limited number of reports are found on diffusion bonding of copper to Ni-based superalloys. In this work, diffusion bonding of a copper alloy to a Ni-based superalloy was successfully performed and the microstructure and mechanical properties of the bonded samples were studied.

2. Experimental

Copper alloy (C18150) and Ni-based superalloy (GH4169) were selected as the base materials in this study. Figure 1 shows the details of the samples joined using a "diffusion bonder" manufactured by the PVA TePla Co. in Germany. The bonder was equipped with a radiation heating system and operated in vacuum level of 1×10^{-3} Pa (i.e. 1×10^{-5} mBar).

The faying surfaces were prepared by conventional grinding techniques with final 1200-grit finish and then polished using 1μm polycrystalline diamond suspension. The specimens were ultrasonically cleaned in the acetone bath and then dried in air before inserting them in the bonding rig.

Previous trials showed that the samples bonded at or below 850 °C have partially bonded joints, judged by the presence of crevices and voids. Bonding at much higher temperatures, *e.g.* +1000 °C, would result in undesirable effects such as grain coarsening in the copper alloy. Therefore, based on the previous optimisation trials, the bonding was carried out at 900°C for 60 min under 10 MPa constant pressure. The samples were first heated up to 750°C at a rate of 12°C/min, then kept for 10 min to ensure entire sample is uniformly heated before further heating up to the bonding temperature. All samples were furnace-cooled to ambient temperature in vacuum. The full bonding cycle is shown in Figure

2. It should be noted that “barrelling” of the copper in the bonded sample, shown in Figure 1, was due to its softening at the bonding temperature and under the applied bonding load. It might be possible to mitigate this side effect by reducing the bonding pressure if post-bonding machining is not possible.

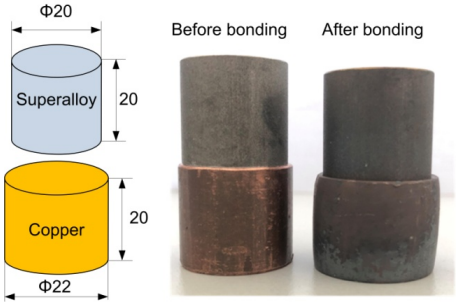

Figure 1. Pre-bonding dimensions (mm) of the samples and effect of bonding cycle on the shape of the copper cylinder.

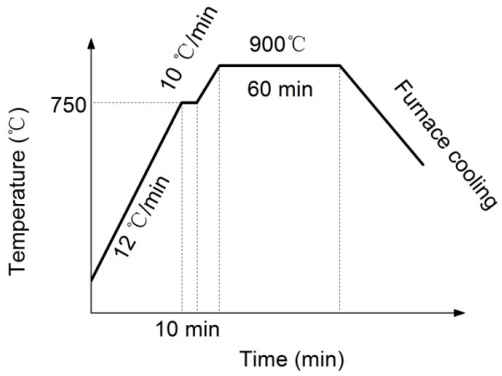

Figure 2. Thermal cycle used to diffusion bond the copper and Ni-based superalloy in this work.

According to the literature reviews and initial examinations, softening of the copper alloy during the bonding process is an important issue. Therefore, a post-bonding heat treatment was needed to restore the mechanical properties of this age-strengthening alloy. Some of the bonded samples were solution treated at 960°C for 60 min followed by rapid cooling and then ageing at 450°C for 3.5 h in vacuum. This is a standard precipitate

hardening process for this family of copper alloys, which could be carried out right after the diffusion bonding cycle provided the furnace is equipped with rapid cooling facility.

The bonded samples were cut along the longitudinal direction and prepared by conventional metallography techniques. Each metallography sample was etched twice using two different etchants. The copper side was etched in a solution of 5 g $FeCl_3$ + 10 ml HCl + 100 ml water, whereas the nickel side was etched by a solution of 1 ml H_2SO_4 + 20 ml HCl + 4g $CuSO_4 \cdot H_2O$ + 20ml water, both at ambient temperature for 20 to 30 s.

The microstructure and composition of each joint interface were examined using optical and scanning electron microscopes (SEM) equipped with an energy dispersive spectrometer (EDS).

Vickers microhardness measurements were conducted within the copper and nickel sides of each joint under 50 g and 200 g constant loads, respectively, all with a 15 s holding time. Longer samples were also bonded and machined for the tensile testing using a universal testing machine - see Figure 3 for more details.

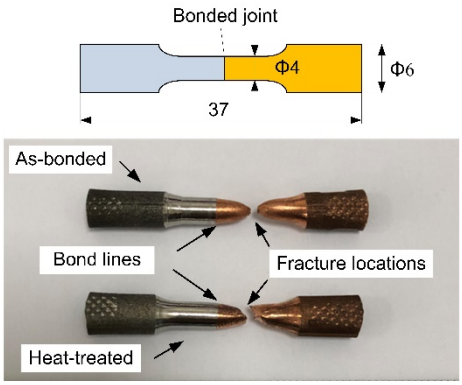

Figure 3. Dimensions and actual tensile-tested samples.

3. Results and discussion

3.1 Microstructural examinations

A typical microstructure of a diffusion-bonded copper/nickel joint is shown in Figure 4a. The

joints were generally free from pores, voids and discontinuities. The backscattered electron (BSE) micrographs of the interface with a higher magnification are shown in Figure 4b. The EDS maps of the Cu, Ni, Cr, Fe and Nb are shown in Figure 5.

The elemental maps show that the inter-diffusion of the elements occurred across the interface, resulting in the formation of an interaction zone. Based on the observed morphological and compositional variations, the interaction or bond zone could be divided into two regions of a uniformly-diffused layer A and a duplex-phase B, as marked in Figure 4b. Both copper and superalloys contain fine precipitates, hence observed speckled microstructures away from the bond zone.

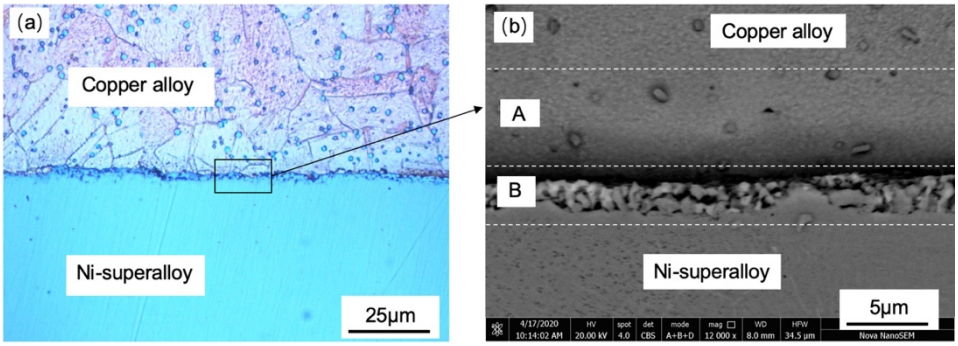

Figure 4. Optical (a) and SEM-BSE (b) micrographs of the copper-superalloy interface in the diffusion bonded sample. The interaction zone was divided into two regions as marked "A" and "B"

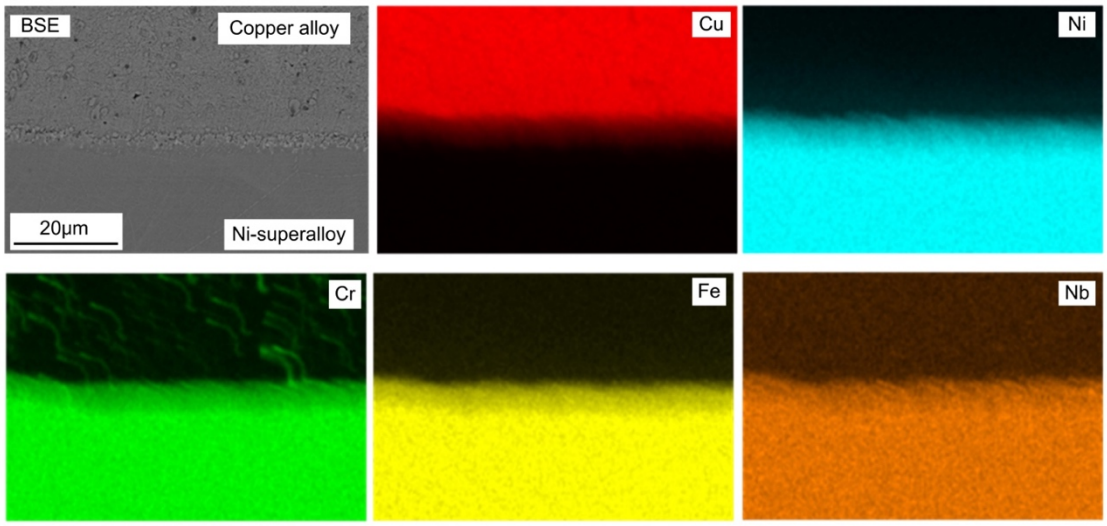

Figure 5. SEM-BSE images and EDS elemental maps show the formation of an interaction zone in a bonded sample.

The elemental maps clearly show the presence of diffusion layers at the joint interface. Nevertheless, a quantitative chemical analysis of the bond zone was carried on several points of interest – see Figure 6 and Table 1. As can be noted in Table 1, the locations marked 1 to 3 in Region A contain mostly Cu as well as small amounts of Ni and Fe. The existence of Ni and Fe in region A showed that the Ni and Fe atoms have diffused into copper alloy and formed Cu solid solution. The locations marked 4 to 6 (darker phases within Region B) are enriched in Cu and contain some elements from the superalloy. These phases could be identified as a Cu-rich solid solution. The locations marked 7 to 9 (lighter phases within Region B) are enriched in Ni and contain the main elements of Ni-based superalloy, as well as small amounts of Cu. These phases could be identified as a Ni-rich solid solution.

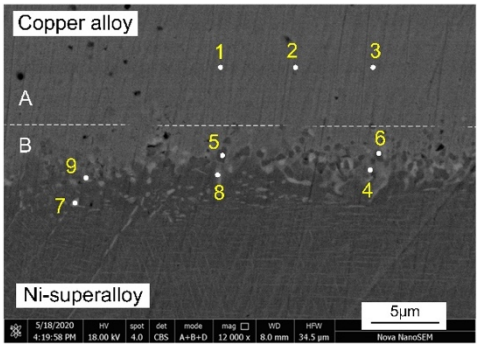

Figure 6. SEM micrographs of the interaction zone showing the locations of EDS analysis.

The binary phase diagram of Cu-Ni system [14] shows Cu and Ni can form a solid solution in any ratios. Moreover, according to the isothermal sections of the ternary phase diagram of Cu-Ni-Cr system [15,16], Cu, Ni and Cr form solid solutions without any intermetallics [16]. Since the bonded samples in this work were cooled rather slowly (*i.e.* quasi-equilibrium condition) the observed lack of any intermetallics in Regions A and B is consistent with the corresponding phase diagram.

Table 1. Chemical composition (wt. %) of the base materials and various locations marked in Figure 6.

Locations	Cu	Ni	Cr	Fe	Ti	Nb	Mo	Zr
C18150	97.50		0.80	0.50				0.10
GH4169		51.08	18.19	17.34	1.22	4.29	2.44	
1	86.73	3.34		0.63				
2	86.01	4.61		0.64				
3	86.32	4.57	0.59	0.78				
4	46.10	17.97	14.14	10.55		1.37	2.07	
5	57.67	13.63	11.07	7.34		1.47		
6	66.08	9.35	9.99	5.39			1.23	
7	3.37	45.45	19.54	17.42	0.73	3.02	2.02	
8	5.76	43.55	17.40	16.65	1.41	5.69	1.95	
9	7.58	39.99	19.55	18.45	0.97	3.24	2.29	

Figure 7 shows the concentration profiles of main elements obtained by an EDS line-scanning across the joint interface. The gradual and smooth changes in the high resolution

EDX line scanning, shown in Figure 7, indicate absence of any intermetallic compounds at Regions A and B within the joint interface. It is also clear that Cu diffused only about 5μm into Ni-based superalloy, whereas Ni diffused a longer distance (about 10μm) into copper alloy. The two sharp peaks in the Cr line are due to pre-existing Cr-rich precipitates within the copper alloy, hence unrelated to the bonding process. Despite the difference in the diffusion range, no Kirkendall voids were found at the joint interfaces examined in this work. The results of this work may appear on contrary to the work by Sabetghadam [5,17], which showed that pure Ni has a shorter diffusion range in pure Cu than Cu in Ni, resulting a large number of Kirkendall voids at the joint interface. Nevertheless, it is plausible that the presence and diffusion of other elements (mainly Cr – see Figure 5) prevented formation of the expected Kirkendall voids. Kemal Aydın [18] studied the direct diffusion bonding of titanium to copper and found that the diffusion range and intensity of Ti in Cu are very different from those of the Cu in Ti.

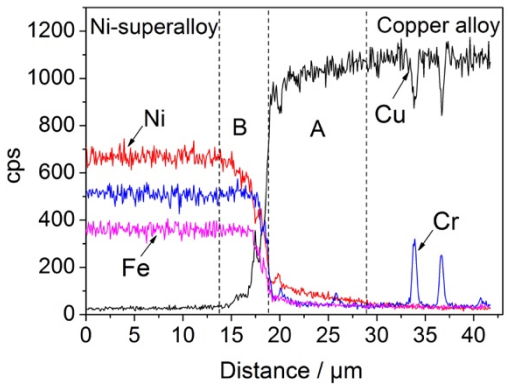

Figure 7. Concentration profiles of main elements across the joint interface.

The effects of bonding and post-bonding heat treatment on the microstructure of the parent copper alloy are shown in Figure 8. It is clear that the as-received copper alloy has elongated grains, caused by cold rolling, whereas the as-bonded sample has finer and equiaxed grains due to high temperature recrystallization during the bonding cycle. Although the heat-treatment had little or no effect on the morphology and size of the grains, the number

of large precipitates is clearly less in the heat-treated sample (Figure 8c) than in the as-received and as-bonded samples (Figures. 8a & 8b). It should be noted that post bonding heat treatment relies on the formation of sub-micron precipitates in the copper matrix during the ageing stage. Such small matrix-strengthening precipitates are not resolvable in the SEM micrographs. This could be due to the dissolution of large globular precipitates during the high temperature heat treatment i.e. at 960°C for 60 min.

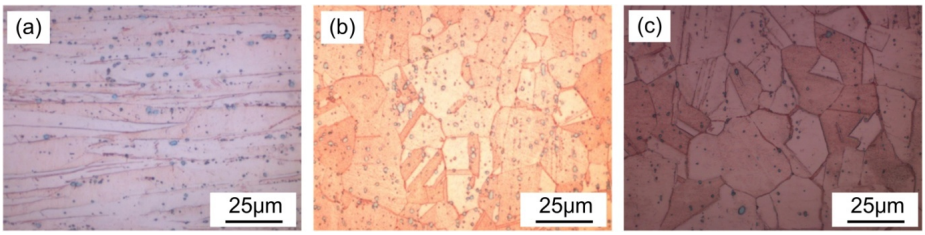

Figure 8. Microstructures of the copper alloy (a) parent material with elongated grains, (b) as-bonded condition with equiaxed grains and (c) after post-bonding heat treatment also with equiaxed grains but less amount of precipitates.

Figure 9 shows the microstructure of the Ni-based superalloy in the as-received, as-bonded and heat-treated conditions. It can be seen that fine γ'/γ'' (Ni_3Al/Ni_xNb) phases are evenly distributed in the γ phase (Ni solid solution) matrix of the as-received superalloy. However, the volumetric ratios of the γ'/γ'' phases were reduced after the bonding cycle and some coarser needle-like phases were nucleated and re-formed on the grain boundaries after complete resolution of the γ'/γ'' phases at the high bonding temperature followed by slow cooling. The γ'/γ'' phases are absent in the heat-treated sample and the needle-like phases are coarsened further.

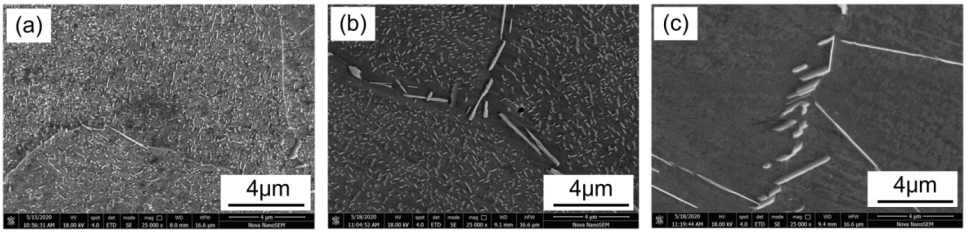

Figure 9. SEM micrographs of the Ni-based superalloy GH4169 used in this work (a) as-received alloy (b) after bonding, (c) after post-bonding heat treatment.

The drastic effect of post-bonding heat treatment on the dissolution of the γ'/γ" phases in GH4169 is completely consistent with the findings of An *et al.* who studied the same superalloy [19]. Figure 10 shows only one-hour exposure of this superalloy to temperatures above 850 °C resulted in annihilation of γ'/γ" precipitates and formation of needle-like phases on the grain boundaries.

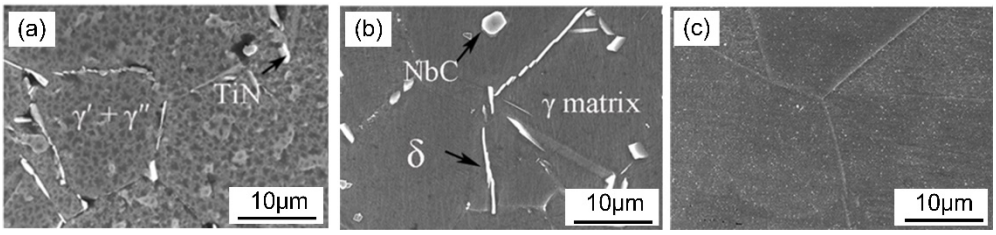

Figure 10. SEM micrographs of the GH4169 superalloys treated at different temperature for 60 min: (a) 850 °C; (b) 950 °C; (c)1050 °C, as reported by An *et.al.* [19]

3.2 Tensile strength and microhardness distribution

Figure 3 in previous section shows that the tensile-tested samples failed in the copper because their bond strengths were above the ultimate tensile strength (UTS) of the as-bonded copper alloy. However, the maximum strength of the as-bonded sample (failed in the copper) was 270MPa, which is only 48% of the strength of the cold-rolled parent alloy (560 MPa). The softening of copper alloy was mostly due to the recrystallization during the bonding process and loss of cold-work hardening. This is fully supported by the microstructures shown in

Figure 8. Concurrently, since CuCrZr alloy is an age-hardening alloy, the strengthening precipitates were also partially dissolved during the bonding process.

The post-bonding treatment reduced the softening effect by restoring the age-hardening effect. The heat-treated sample also failed in the copper alloy but its tensile strength was 429MPa, which is 77% of the cold-rolled parent alloy. Nevertheless, all joints made in this work proved to be "fail-safe" in both as-bonded and heat-treated conditions.

Figure 11 shows the microhardness distributions across the inter-diffusion zone in various samples. It could be seen that the hardness of both copper alloy and Ni-based superalloy decreased significantly after bonding process compared to their parent materials. The softening of copper alloy, which is more detrimental than softening of the superalloy, was attributed to the loss of both cold-work and age-hardening effects during the bonding at a high temperature. Meanwhile, the softening of Ni-based superalloy was most likely due to the dissolution of fine γ'/γ" phases (see the microstructure changes in Figure 9)

To restore the strength of copper alloy, *i.e.* the weakest part of the sample, the bonded sample were heat treated under the conditions mentioned above. As expected, and consistent with the tensile test results, the hardness of copper alloy was restored to some extent. Nevertheless, a further decrease of hardness was observed on the Ni-based superalloy, which could be attributed to the further dissolution of the strengthening precipitates in the matrix (see the microstructure changes in Figure 9c). The softening of copper alloy is indeed a drawback of the diffusion bonding. However, it might be possible to develop a multiple-stage heat treatment to restore mechanical properties of both parent alloys.

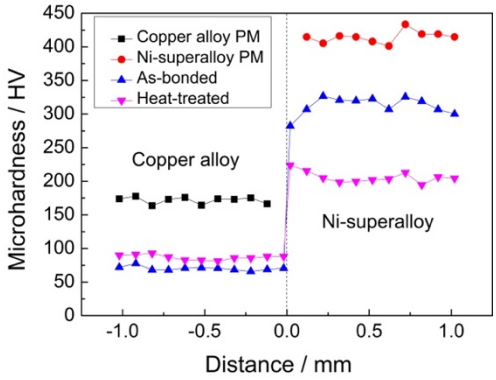

Figure 11. Microhardness distributions of the as-bonded and heat-treated samples compared to those of the as-received parent alloys (PM).

4. Conclusions

Diffusion bonding of a copper alloy to a Ni-based superalloy was performed in vacuum. Based on the microstructural examinations and mechanical testing, the following main conclusions can be made:

1) Sound joints between the copper alloy and Ni-based superalloy, free from pores, voids and discontinuities were obtained by diffusion bonding at 900°C for 60 min under 10 MPa constant pressure.
2) Inter-diffusion of atoms across the interface led to the formation of an interaction zone comprising of two solid solution regions and no intermetallic compounds were found at or around the joint interface.
3) All tensile tested samples, both the as-bonded and heat-treated ones, failed in the copper alloy and away from the joints.
4) The maximum tensile strengths of the as-bonded and heat-treated samples were 48% and 77% of that of the parent copper alloy, respectively.
5) An age-hardening process partially restored the strength and hardness of the bonded copper alloy but adversely softened the Ni-based superalloy further.

Acknowledgments

The help for providing the bonding machine from Mr Kang Yu is highly appreciated. The authors also would like to acknowledge the technical assistance and helpful discussion received from Mr Cheng Xu, Mr Chunsheng Sha and Miss Jing Jin.

Disclosure statement

No potential conflict of interest was reported by the authors.

Funding

This work was supported by the National Natural Science Foundation of China (51905348). The first author was sponsored by Shanghai Rising-Star Program (20QB1402700).

References

[1] Moreschi L., Pizzuto A, Alessandrini I, Agostini M, Visca E, Merola M. Fabrication of mock-up with Be armour tiles diffusion bonded to the CuCrZr heat sink. Fusion Eng Des 2001;56–57:321–4. https://doi.org/10.1016/s0920-3796(01)00348-9.

[2] Goods SH, Puskar JD. Solid state bonding of CuCrZr to 316L stainless steel for ITER applications. Fusion Eng Des 2011;86:1634–8. https://doi.org/10.1016/j.fusengdes.2010.12.051.

[3] Lee HS. Diffusion bonding of metal alloys in aerospace and other applications. Woodhead Publishing Limited; 2011. https://doi.org/10.1016/B978-1-84569-532-3.50010-1.

[4] Lee HS, Yoon JH, Yoo JT, Yi YM. A study on diffusion bonding of steel and copper alloy. Materwiss Werksttech 2011;42:985–9. https://doi.org/10.1002/mawe.201100856.

[5] Sabetghadam H, Hanzaki AZ, Araee A. Diffusion bonding of 410 stainless steel to copper using a nickel interlayer. Mater Charact 2010;61:626–34. https://doi.org/10.1016/j.matchar.2010.03.006.

[6] Batra IS, Kale GB, Saha TK, Ray AK, Derose J, Krishnan J. Diffusion bonding of a Cu-Cr-Zr alloy to stainless steel and tungsten using nickel as an interlayer. Mater Sci Eng A 2004;369:119–23. https://doi.org/10.1016/j.msea.2003.10.296.

[7] Singh KP, Patel A, Bhope K, Khirwadkar SS, Mehta M. Optimization of the diffusion bonding parameters for SS316L/CuCrZr with and without Nickel interlayer. Fusion Eng Des 2016;112:274–82. https://doi.org/10.1016/j.fusengdes.2016.09.004.

[8] Ghosh SK, Chatterjee S. On the direct diffusion bonding of titanium alloy to stainless steel. Mater Manuf Process 2010;25:1317–23. https://doi.org/10.1080/10426914.2010.520793.

[9] Yuan X, Tang K, Deng Y, Luo J, Sheng G. Impulse pressuring diffusion bonding of a copper alloy to a stainless steel with/without a pure nickel interlayer. Mater Des 2013;52:359–66. https://doi.org/10.1016/j.matdes.2013.05.057.

[10] Xiong JT, Xie Q, Li JL, Zhang FS, Huang WD. Diffusion bonding of stainless steel to copper with tin bronze and gold interlayers. J Mater Eng Perform 2012;21:33–7. https://doi.org/10.1007/s11665-011-9870-y.

[11] Srikanth V, Laik A, Dey GK. Joining of stainless steel 304L with Zircaloy-4 by diffusion bonding technique using Ni and Ti interlayers. Mater Des 2017;126:141–54. https://doi.org/10.1016/j.matdes.2017.04.037.

[12] Singh KP, Bhavsar R, Patel K, Khirwadkar SS, Patel A, Bhope K. Joining of WCu-CuCrZr coupon materials by diffusion bonding technique for divertor plasma facing components. Fusion Eng Des 2017;121:272–81. https://doi.org/10.1016/j.fusengdes.2017.08.003.

[13] Ziegelheim J, Hiraki S, Ohsawa H. Diffusion bondability of similar/dissimilar light metal sheets. J Mater Process Technol 2007;186:87–93. https://doi.org/10.1016/j.jmatprotec.2006.12.020.

[14] Wang CP, Liu XJ, Jiang M, Ohnuma I, Kainuma R, Ishida K. Thermodynamic database of the phase diagrams in copper base alloy systems. J Phys Chem Solids 2005;66:256–60. https://doi.org/10.1016/j.jpcs.2004.08.037.

[15] Ikoma T, Kajihara M. Thermodynamic evaluation of phase equilibria in the ternary Cu-Cr-Ni system. Mater Sci Eng A 2006;437:293–300. https://doi.org/10.1016/j.msea.2006.08.032.

[16] Qiu C, Hu B, Zhou J, Wu P, Liu Y, Wang C, et al. The phase equilibria of the Cu–Cr–Ni and Cu–Cr–Ag systems: Experimental investigation and thermodynamic modeling. Calphad Comput Coupling Phase Diagrams Thermochem 2020;68:101734. https://doi.org/10.1016/j.calphad.2019.101734.

[17] Sabetghadam H, Zarei Hanzaki A, Araee A, Hadian A. Microstructural evaluation of 410 SS/Cu diffusion-bonded joint. J Mater Sci Technol 2010;26:163–9. https://doi.org/10.1016/S1005-0302(10)60027-8.

[18] Aydin K, Kaya Y, Kahraman N. Experimental study of diffusion welding/bonding of titanium to copper. Mater Des 2012;37:356–68. https://doi.org/10.1016/j.matdes.2012.01.026.

[19] An XL, Zhang B, Chu CL, Zhou L, Chu PK. Evolution of microstructures and properties of the GH4169 superalloy during short-term and high-temperature processing. Mater Sci Eng A 2019;744:255–66. https://doi.org/10.1016/j.msea.2018.12.019.